

## Direct patterning of functional interfaces in oxide heterostructures

N. Banerjee, M. Huijben,<sup>a)</sup> G. Koster, and G. Rijnders

Faculty of Science & Technology and MESA<sup>+</sup> Institute for Nanotechnology, University of Twente,  
P.O. Box 217, 7500 AE, Enschede, The Netherlands

(Received 23 November 2011; accepted 5 January 2012; published online 23 January 2012)

We report on the direct patterning of high-quality structures incorporating the LaAlO<sub>3</sub>-SrTiO<sub>3</sub> interface by an epitaxial-liftoff technique avoiding any reactive ion beam etching. Detailed studies of temperature dependent magnetotransport properties were performed on the patterned heterostructures with variable thickness of the LaAlO<sub>3</sub> layer and compared to their unstructured thin film analogues. The results demonstrate the conservation of the high-quality interface properties in the patterned structures enabling future studies of low-dimensional confinement on high mobility interface conductivity as well as interface magnetism. © 2012 American Institute of Physics. [doi:10.1063/1.3679379]

The remarkable observation of a high-mobility electron gas at the interface between the band insulators SrTiO<sub>3</sub> (STO) and LaAlO<sub>3</sub> (LAO)<sup>1</sup> has initiated extensive research into the exceptional properties of this two dimensional system. Several fundamental studies have demonstrated various interesting interface properties, such as superconductivity<sup>2</sup> and magnetism.<sup>3</sup> To develop these unique interfaces into useful technologies, high-quality devices have to be fabricated from thin films by reproducible structurization techniques. Reactive Ar-ion etching has been used extensively to produce controlled structures in various materials. However, the implementation of this technique for LAO-STO interfaces is hampered due to the formation of oxygen vacancies, which would result in a conducting surface layer at the STO substrate.<sup>4</sup> Alternatively, previous studies have used UV lithography to create measurement structures by combining a hard mask of amorphous LaAlO<sub>3</sub> (Ref. 5) or AlO<sub>x</sub> (Ref. 6) and pulsed laser deposition (PLD). The disadvantage of this technique is the presence of the hard mask material on the surface of the final device. Finally, scanning probe microscopy has been applied to form structures down to the nanoscale.<sup>7,8</sup> However, the disadvantage of this latter technique is the degradation of the created patterns in ambient conditions. To date, there has not been a demonstration of a reproducible technique to fabricate well-controlled structures without any of the above mentioned disadvantages.

Here, we present the direct patterning of high-quality structures incorporating the LAO-STO interface by an epitaxial-liftoff technique without performing any reactive ion beam etching. The patterned structures incorporating the LAO-STO interface exhibited high quality interfacial properties which have previously been measured only in thin film samples. Detailed studies of temperature dependent magnetotransport properties were performed on the patterned heterostructures with variable thickness of the LAO layer and compared to their unstructured thin film analogues. The results demonstrate the conservation of the high-quality interface properties in the patterned structures enabling future studies on the low-dimensional confinement on high

mobility interface conductivity as well as interface magnetism. At the same time, the development of this patterning method provides a first step in integrating high quality oxide interfaces exhibiting unique two-dimensional properties with other essential components on the same substrate crystal for device applications.

In order to fabricate these structures, the following steps were used: initially, a thin (~30 nm) layer of amorphous aluminum oxide was deposited on a TiO<sub>2</sub>-terminated STO (001) single crystal substrate<sup>9</sup> by PLD. A KrF excimer laser was applied to ablate a single crystalline AlO<sub>x</sub> target at a repetition rate of 5 Hz and a laser fluence of ~1.5 J cm<sup>-2</sup>. During growth, the substrate was held at room temperature in an oxygen environment of 0.15 mbar. In the first step, the amorphous aluminum oxide was subsequently subjected to a

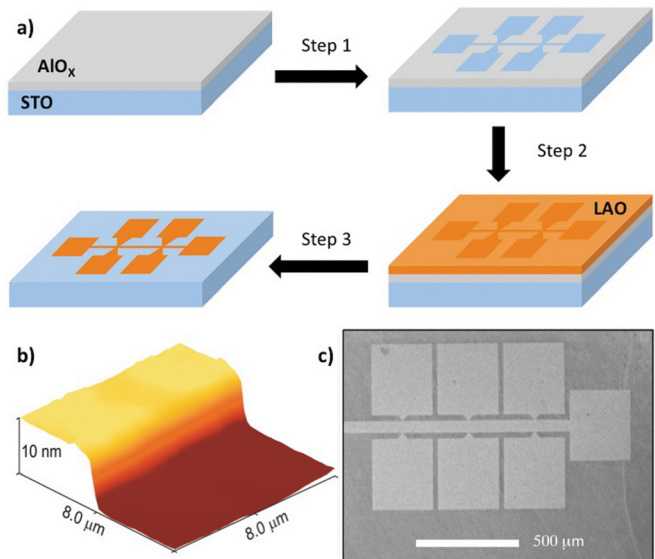


FIG. 1. (Color online) (a) Schematic representation of the patterning process to create well-defined structures incorporating a LAO/STO interface. Step 1: photolithography to produce a TiO<sub>2</sub>-terminated STO substrate covered with amorphous aluminum oxide with structured openings; Step 2: growth of LAO layer by PLD; Step 3: lift-off of aluminum oxide layer with LAO layer on top. (b) 3D representation of an atomic force micrograph of the edge of the structure. (c) Scanning electron micrograph displaying the final Hall bars incorporating a LAO/STO interface.

<sup>a)</sup>Electronic mail: m.huijben@utwente.nl.

photolithographic process in which a negative mask with hall-bar structures was UV illuminated, see Fig. 1. The used photolithographic developer solution (OPD 4262) for the positive resist is a basic solution, and hence, it reacts also with exposed aluminum oxide to form water-soluble alkali-metal aluminates. All photoresist was removed subsequently using organic solvents. This simple process creates a negative mimic of the mask into amorphous  $\text{AlO}_x$  layer, which yields a  $\text{TiO}_2$ -terminated STO substrate covered with amorphous aluminum oxide with structured openings. In the second step, thin LAO films of different thicknesses were grown by PLD on these pre-patterned substrates at  $800^\circ\text{C}$  and  $10^{-3}$  mbar  $\text{O}_2$  from a single crystalline LAO target at a repetition rate of 1 Hz and a laser fluence of  $\sim 1.3 \text{ J cm}^{-2}$ , similar to previous studies.<sup>3,10</sup> After growth, the samples were slowly cooled down to room temperature at deposition pressure without any extra annealing step. In the third and final step, the lift-off process was performed using a 4M aqueous NaOH solution in which the aluminum oxide dissolves as water soluble sodium aluminate removing the LAO layer on top as well. The final result is a well-defined structure incorporating a LAO/STO interface, which is very stable over a long period of time in ambient conditions, without any surface contamination of the original mask. To compare the electrical transport properties of patterned structures to their unstructured thin film analogues, samples with identical deposition conditions were grown on  $\text{TiO}_2$ -terminated STO (001) substrates. The patterned Hall bars (width:  $50 \mu\text{m}$ , length:  $300 \mu\text{m}$ ) in the structured samples, as well as the thin films, were wirebonded with Al wire to form Ohmic contacts for electrical transport measurement.

The temperature dependence of the sheet resistance for both thin (10 u.c. (unit cells)) and thick (26 u.c.) LAO layers is shown in Fig. 2, in which can be clearly observed that LAO/STO interfaces in thin films and Hall bars provide very similar transport properties. It is evident that thick LAO layers in both Hall bars and thin films show an upturn in sheet resistance at low temperatures, which is in good agreement with previous reports.<sup>3,11</sup> In there, a suggestive explanation for the observed logarithmic temperature dependence of the sheet resistance upturn was the Kondo effect, which describes the interplay between localized magnetic moments and mobile charge carriers.<sup>3</sup> The sheet resistance can be

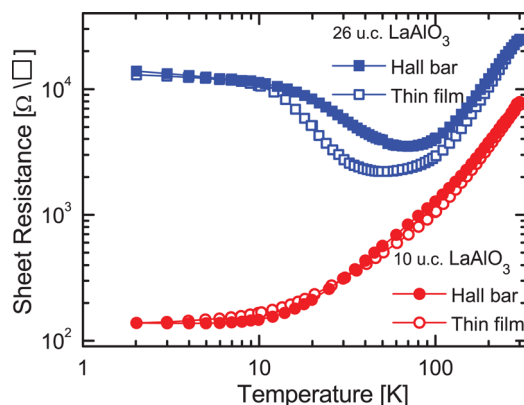


FIG. 2. (Color online) Temperature dependent sheet resistance of the conducting  $\text{LaAlO}_3/\text{SrTiO}_3$  interface for different  $\text{LaAlO}_3$  layer thicknesses of 10 and 26 u.c. situated in thin films and Hall bars.

described in this temperature range ( $\sim 5\text{--}50 \text{ K}$ ) by  $R_S = a \ln(T/T_{eff}) + bT^2 + cT$ ,<sup>5</sup> where  $T_{eff}$  is an effective crossover temperature scale, and where the  $T^2$  and  $T^5$  terms are suggestive of electron-electron and electron-phonon scattering, relevant at higher temperatures. Saturation of the logarithmic term is observed below  $\sim 5 \text{ K}$ . Although, in general, similar transport properties are observed for thin films and Hall bars, fitting of the measurement results demonstrates small variations in  $T_{eff}$  of  $\sim 50 \text{ K}$  and  $\sim 70 \text{ K}$ , for respectively thin films and Hall bars. For thin LAO layers, metallic behavior down to  $2 \text{ K}$  is observed in agreement with previous reports.<sup>11,12</sup>

The temperature dependencies of the corresponding sheet carrier density  $n_S$  and carrier mobility  $\mu$  are shown in Fig. 3, which were deduced from measurements of the Hall coefficient  $R_H$ , using  $n_S = -1/R_H e$ . Also here, the structuring technique induced no measurable effect on the transport properties as similar results are observed for thin films and Hall bars. All samples exhibited thermally activated carriers comparable to previous observations<sup>13</sup> with the room temperature sheet carrier density decreasing with increasing LAO thickness.<sup>11</sup> At low temperatures, the thick samples show an enhancement in sheet carrier density together with a decrease in carrier mobility in good agreement with previous reports for thin films.<sup>3,11</sup> There, the inadequacy of a single band model for the data fitting at low temperatures was suggested as a cause for the observed effects. Thin samples display a low carrier density of  $\sim 1 \times 10^{13} \text{ cm}^{-2}$  and a high carrier mobility of  $\sim 4000 \text{ cm}^2 \text{ V}^{-1} \text{ s}^{-1}$ . These observations of high carrier mobilities in structured Hall bars are

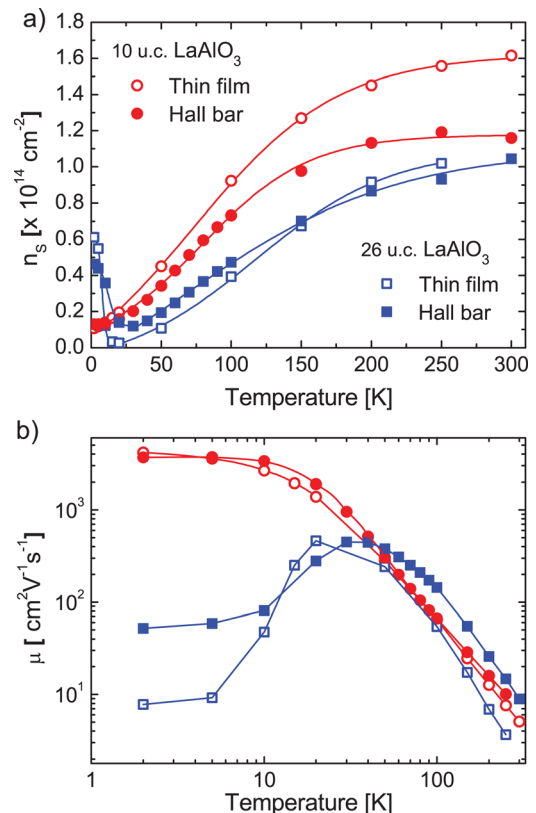


FIG. 3. (Color online) Temperature dependent carrier density  $n_S$  (a) and carrier mobility  $\mu$  (b) of the conducting  $\text{LaAlO}_3/\text{SrTiO}_3$  interface for different  $\text{LaAlO}_3$  layer thicknesses of 10 and 26 u.c. situated in thin films and Hall bars.

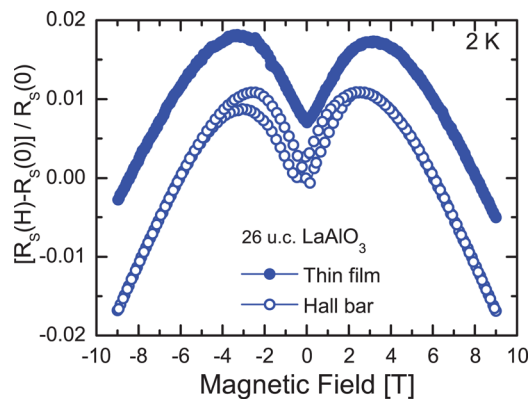


FIG. 4. (Color online) Magnetoresistance of the conducting  $\text{LaAlO}_3/\text{SrTiO}_3$  interface for thick (26 u.c.)  $\text{LaAlO}_3$  layer thicknesses situated in thin films and Hall bars. Thin film data are shifted upwards for clarity.

comparable to reports on thin films,<sup>14</sup> but these Hall bars enable future detailed studies on the physics of these interfaces in low-dimensional structures.

In addition to the interface induced conductivity, magnetic effects at low temperatures with large negative magnetoresistance values have been reported for the LAO-STO interface.<sup>3</sup> Subsequent study of the LAO thickness dependence demonstrated the manifestation of this remarkable effect only for thick ( $\sim 25$  u.c.) LAO layers.<sup>11</sup> In good agreement to those previous reports, our thick samples show large negative magnetoresistance for large magnetic fields at 2 K in both thin films and Hall bars, see Fig. 4, while thin samples display a purely positive magnetoresistance over the total magnetic field range. The magnetoresistance was defined as the change in the sheet resistance with respect to the zero field resistance  $[R_S(H) - R_S(0)]/R_S(0)$ . Fig. 4 clearly shows the occurrence of large negative magnetoresistance at 2 K for both thin films and Hall bars of  $\sim 2\%$ . Strikingly, the sample with structured Hall bars shows hysteresis behavior already at 2 K, while for thin films this has only been observed<sup>3</sup> at much lower temperatures of 0.3 K. Magnetoresistance hysteresis is usually indicative of ferromagnetic domain formation in which domains change polarity above a certain coercive field. Domain formation typically creates a remanence in the signal when crossing zero-field, providing a butterfly shape of the magnetoresistance curve. An additional suppression around zero-field seems to occur, which could suggest additional spin/domain reorientation effects, such as observed in granular and spin-valve giant magnetoresistance systems and the Kondo effect in quantum dots in the presence of ferromagnetism.<sup>15</sup>

In conclusion, we have studied the electrical transport properties of LAO-STO interfaces in patterned structures and compared them to their unstructured thin film analogues.

This study was enabled by the development of a direct patterning technique, consisting of a 3-step process avoiding reactive ion etching, to create structures containing functional interfaces. The disadvantages of previous structuring techniques have been prevented and the resulting structures exhibit interface phenomena previously only observed in unstructured thin film samples. Our direct patterning method enables now the detailed study of low-dimensional confinement on high mobility interface conductivity in heterostructures with thin LAO layers as well as interface magnetism in heterostructures with thick LAO layers. At the same time, the development of this patterning method provides a first step in integrating high quality oxide interfaces exhibiting unique two-dimensional properties with other essential components on the same substrate crystal for device applications.

This research was carried out under project number M62.2.08SDMP21 in the framework of the Industrial Partnership Program on Size Dependent Material Properties of the Materials innovation institute M2i ([www.m2i.nl](http://www.m2i.nl)) and the Foundation of Fundamental Research on Matter (FOM) ([www.fom.nl](http://www.fom.nl)), which is part of the Netherlands Organisation for Scientific Research ([www.nwo.nl](http://www.nwo.nl)).

<sup>1</sup>A. Ohtomo and H. Y. Hwang, *Nature* **427**, 423 (2004).

<sup>2</sup>N. Reyren, S. Thiel, A. D. Caviglia, L. Kourkoutis, G. Hammerl, C. Richter, C. W. Schneider, T. Kopp, A. S. Ruetschi, D. Jaccard *et al.*, *Science* **317**, 1196 (2007).

<sup>3</sup>A. Brinkman, M. Huijben, M. van Zalk, J. Huijben, U. Zeitler, J. C. Maan, W. G. van der Wiel, G. Rijnders, D. H. A. Blank, and H. Hilgenkamp, *Nature Mater.* **6**, 493 (2007).

<sup>4</sup>D. W. Reagor and V. Y. Butko, *Nature Mater.* **4**, 593 (2005).

<sup>5</sup>C. W. Schneider, S. Thiel, G. Hammerl, C. Richter, and J. Mannhart, *Appl. Phys. Lett.* **89**, 122101 (2006).

<sup>6</sup>C. Bell, S. Harashima, Y. Kozuka, M. Kim, B. G. Kim, Y. Hikita, and H. Y. Hwang, *Phys. Rev. Lett.* **103**, 226802 (2009).

<sup>7</sup>C. Cen, S. Thiel, G. Hammerl, C. W. Schneider, K. E. Andersen, C. S. Hellberg, J. Mannhart, and J. Levy, *Nature Mater.* **7**, 298 (2008).

<sup>8</sup>C. Cen, S. Thiel, J. Mannhart, and J. Levy, *Science* **323**, 1026 (2009).

<sup>9</sup>G. Koster, B. L. Kropman, G. J. H. M. Rijnders, D. H. A. Blank, and H. Rogalla, *Appl. Phys. Lett.* **73**, 2920 (1998).

<sup>10</sup>M. Huijben, A. Brinkman, G. Koster, G. Rijnders, and D. H. A. Blank, *Adv. Mater.* **21**, 1665 (2009).

<sup>11</sup>C. Bell, S. Harashima, Y. Hikita, and H. Y. Hwang, *Appl. Phys. Lett.* **94**, 222111 (2009).

<sup>12</sup>R. Pentcheva, M. Huijben, K. Otte, W. E. Pickett, J. E. Kleibeuker, J. Huijben, H. Boschker, D. Kockmann, W. Siemons, G. Koster *et al.*, *Phys. Rev. Lett.* **104**, 166804 (2010).

<sup>13</sup>M. Huijben, G. Rijnders, D. H. A. Blank, S. Bals, S. Van Aert, J. Verbeeck, G. Van Tendeloo, A. Brinkman, and H. Hilgenkamp, *Nature Mater.* **5**, 556 (2006).

<sup>14</sup>A. D. Caviglia, S. Gariglio, C. Cancellieri, B. Sacépé, A. Fête, N. Reyren, M. Gabay, A. F. Morpurgo, and J. M. Triscone, *Phys. Rev. Lett.* **105**, 236802 (2010).

<sup>15</sup>A. N. Pasupathy, R. C. Bialczak, J. Martinek, J. E. Grose, L. A. K. Donev, P. L. McEuen, and D. C. Ralph, *Science* **306**, 86 (2004).